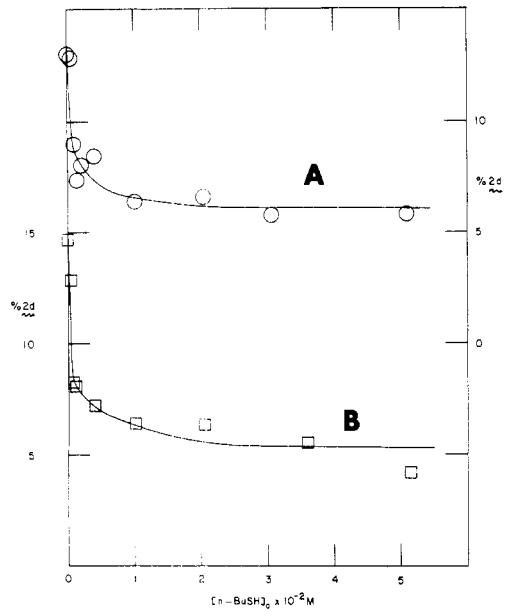

Figure 3. Effect of $[n\text{-BuSH}]_0$ on the yield of **2d** obtained from irradiation of **1d** in DME: A, scale at right, run 1; B, scale at left, run 2. $[\mathbf{1d}]_0$ was 2.0×10^{-3} M.

reagent solution was prepared as directed. Ten milliliters of this solution and 10 mL of the test solution were mixed and warmed for 10 min at 50 °C. The yellow color which developed was assayed at 412 nm. Formaldehyde was detected in this way in DME which had been distilled over lithium aluminum hydride (LAH). Therefore, DME was distilled over a mixture of sodium bisulfite and sodium sulfite. The distillate was free of formaldehyde but had a bad odor (H_2S?). Therefore, it was redistilled over LAH. The first fraction again gave a strong positive response to Hantzsch's reagent. The second fraction gave a weak response while the third gave a negative response. The third distillate was used in photolysis experiments and as a blank.

For assaying formaldehyde which was formed in a photolysis, 10 mL of a 2.07×10^{-3} M solution of **1d** was degassed by three freeze–thaw cycles and irradiated for 60 min in the Rayonet reactor while being stirred magnetically. The solvent from the irradiated solution was pumped off at room temperature and collected in a trap cooled in liquid N_2. The trapped distillate was warmed to room temperature and assayed with Hantzsch's reagent. The concentration of formaldehyde was assayed as 3.94×10^{-5} M. A 10-mL aliquot of the solvent, DME, tested out as being free from formaldehyde, but when 50 mL of DME was irradiated and worked up as with the solution of **1d**, formaldehyde was detected and assayed as being 5.88×10^{-6} M. The amount of formaldehyde obtained from **1d**, corrected for the blank, was 1.9% of the **1d** used.

Registry No. **1b**, 74763-65-8; **1d**, 26190-53-4; **1e**, 26190-49-8; **1f**, 26190-51-2; **2b**, 74763-66-9; **2d**, 74763-67-0; **2e**, 30724-66-4; **2f**, 51596-02-2; **3e**, 623-08-5; **3f**, 10541-82-9; **4f**, 74763-68-1; **5b**, 1601-98-5; **5d**, 74763-69-2; **5e**, 501-60-0; **5f**, 7250-68-2; **6b**, 19717-43-2; **6d**, 74763-70-5; **6e**, 637-47-8; **6f**, 19672-25-4; 1-(*p*-bromophenyl)-1-methylhydrazine, 74763-71-6; 1-(*p*-tolyl)-1-methylhydrazine, 24006-21-1; 1-[*p*-(ethoxycarbonyl)phenyl]-1-methylhydrazine, 74763-72-7; *p*-nitrotoluene, 99-99-0; *p*-bromoaniline, 106-40-1; ethyl *p*-aminobenzoate, 94-09-7; *p*-toluidine, 106-49-0.

Frontier-Controlled Pericyclic Reactions of Powerful Electron-Attracting Cyclic Dienones and Diazadienones with 1*H*-Azepine: Molecular Structures of Cycloadducts and Some Comments

Kazunobu Harano, Masami Yasuda, Takashi Ban, and Ken Kanematsu*

Institute of Synthetic Organic Chemistry, Faculty of Pharmaceutical Sciences, Kyushu University 62, Maidashi, Higashi-ku, Fukuoka 812, Japan

Received July 29, 1980

Pericyclic reactions of 2,5-bis(methoxycarbonyl)-3,4-diphenylcyclopentadienone (**1a**) and 2,5-diphenyl-3,4-diazacyclopentadienone (**1d**) with *N*-(ethoxycarbonyl)azepine (**2a**) were investigated. For **1a**, novel exo $[4 + 6]\pi$ and anti endo $[2 + 4]\pi$ cycloadducts were obtained, whereas for **1d**, only the anti endo $[2 + 4]\pi$ cycloadduct was obtained. These structures were verified by X-ray crystallography. The anti endo $[2 + 4]\pi$ cycloadduct was found to be formed via Cope rearrangement of the endo $[4 + 2]\pi$ cycloadduct by UV spectrometry. Compounds **1** are found to have high reactivities toward **2a**, and the selectivities were discussed in terms of frontier molecular orbital theory, indicating that **1** is a useful 4π component with inverse electron demand.

Pericyclic syntheses are very valuable for the high stereo-, regio-, and periselective controls they could provide for a logical assembling of molecules, especially highly strained cage compounds which either are available or are not available from natural sources.

In the past decade, the pericyclic reactions of conjugated medium-ring polyenes have aroused considerable interest and much effort has been made to establish their capability for cycloaddition. In general, cycloaddition reactions of medium-ring unsaturated compounds with electron-deficient dienophiles are extensively studied.

On the other hand, it is well-known that cyclopentadienone and its analogues are reactive and versatile diene components in Diels–Alder reactions.[1] We have also

Chart I

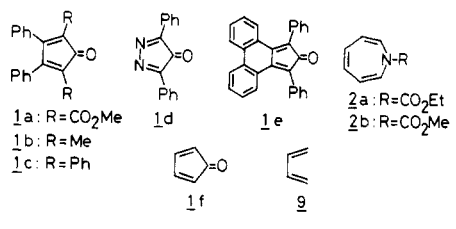

elucidated that phencyclone (2-oxo-1,3-diphenyl-2*H*-cyclopenta[*l*]phenanthrene, **1e**; see Chart I) shows high reactivity and selectivity toward various olefins and conjugated medium-ring polyenes on the basis of MO calculations and kinetic evidence, indicating that the reaction can be rationalized as a "neutral" Diels–Alder reaction where both electron-releasing and -attracking substituents

(1) Hoffmann, R.; Woodward, R. B. *J. Am. Chem. Soc.* **1965**, *87* 4388–4389; *Angew. Chem.* **1969**, *81*, 797–869.

0022-3263/80/1945-4455$01.00/0

Table I. FMO Energy Levels of Cyclopentadienones 1, *N*-(Methoxycarbonyl)azepine (2b), and Butadiene (9) Calculated by PPP MO[11] and CNDO/2 MO[12] Methods

		1a	1b	1c	1d	1e	1f	2b	9
PPP MO	LUMO[a]	−3.97	−3.58	−3.61	−3.92	−3.89	−3.48	−2.29	−1.32
	HOMO[a]	−9.82	−9.23	−8.90	−9.60	−8.50	−10.2	−8.52	−9.87
CNDO/2 MO	LUMO[a]	0.064[b]	0.656	0.688	−0.052[b]	−0.223	0.672	2.51	3.43
	HOMO[a]	−11.5[b]	−10.6	−10.6	−10.9[b]	−9.50	−13.0	−10.5	−13.0

[a] In electron volts. [b] The optimum geometries of 1a and 1d were determined by the X-ray results of the corresponding anti endo [2 + 4]π cycloadducts (5a, 5d).

Scheme I

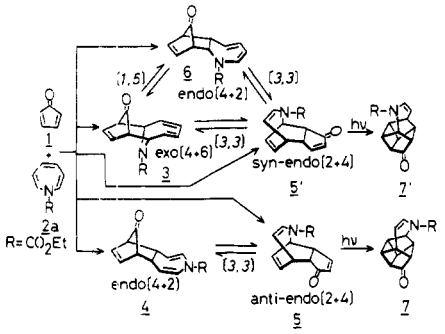

on the dienophile accelerate the reaction rate.

On the basis of the concept of the highest occupied molecular orbital (HOMO) and the lowest unoccupied molecular orbital (LUMO) relationships of the frontier-controlled pericyclic reaction, we have considered that introduction of strong electron-attracting substituents in the cyclopentadienone, which causes a decrease of the LUMO energy of the parent molecule and enhancement of the reactivity of the cyclopentadienone, will accelerate the pericyclic reaction of medium-ring unsaturated compounds such as an electron-releasing 1*H*-azepine.

In this connection, we have recently communicated the pericyclic reaction between 2,5-bis(methoxycarbonyl)-3,4-diphenylcyclopentadienone (**1a**) and *N*-(ethoxycarbonyl)azepine (**2a**).[2] These results are discussed here in detail in comparison with previous work[3-6] and with further additional data that we have obtained.

Results

Theoretical Expectations. The possible reaction pathways outlined in Scheme I are presented, which involve all of the thermally allowed cycloadducts from cyclopentadienone and 1*H*-azepine by either a direct or an indirect pathway. On the other hand, the photochemical [2 + 2]π cycloaddition should provide the highly strained cage compounds[7] of current interest as a models for chemical storage of solar energy[8] or in the fields of pharmacology and biochemistry.[9]

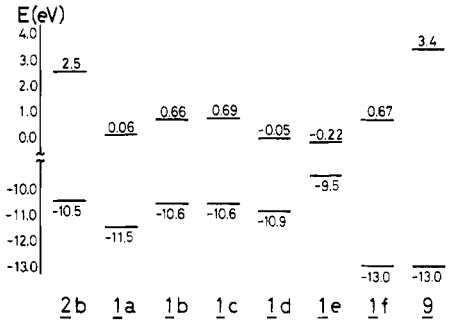

Figure 1. Calculated FMO energy levels by CNDO/2 MO method.

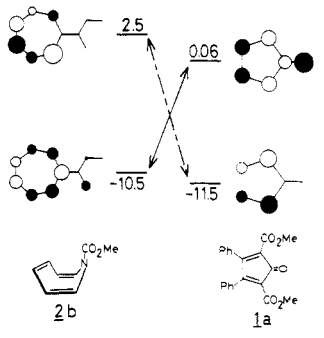

Figure 2. FMO energy levels and coefficients by CNDO/2 MO calculations.

For the exact prediction, the CNDO/2 MO calculations were performed on the model near the actual geometry. A complete description of the geometries of cyclopentadienones used in the calculations is given in the previous paper[4] in this series.

The molecular structure of *N*-(methoxycarbonyl)azepine (**2b**) used for CNDO/2 MO calculations is depicted in Figure 3: the three-dimensional coordinates of **2b** are composed by using the X-ray results from the *N*-brosylazepine and iron tricarbonyl complexes of 1*H*-azepine.[10]

The calculations reported here were carried out by PPP MO[11] and CNDO/2 MO[12] methods and are summarized in Table I.

As shown in Figure 1, in the light of the very low LUMO, cyclopentadienone should be more readily trapped by dienophiles than by other 4π components, e.g., butadiene (**9**).

The CNDO/2 MO calculation (Figure 1) indicates a 0.7-eV lowering of the LUMO for **1a** as compared to those

(2) Harano, K.; Ban, T.; Yasuda, M.; Kanematsu, K. *Tetrahedron Lett.* **1979**, 1599–1602.
(3) Mukai, T.; Yamashita, Y.; Sukawa, H. *Chem. Lett.* **1975**, 423–426.
(4) Yasuda, M.; Harano, K.; Kanematsu, K. *J. Org. Chem.* **1980**, *45*, 659–664.
(5) Yasuda, M.; Harano, K.; Kanematsu, K. *J. Org. Chem.* **1980**, *45*, 2368–2372. In contrast to the mild reaction conditions for **1a**, the cycloadduct **10** underwent rearrangement to the Cope product only when heated to above 100 °C.
(6) Abramovitch, R. A.; Knaus, G. N. *J. Chem. Soc., Chem. Commun.* **1974**, 238–239.
(7) Harano, K.; Ban, T.; Yasuda, M.; Osawa, E.; Kanematsu, K., submitted for publication in *J. Am. Chem. Soc.*
(8) Mukai, T.; Yamashita, Y. *Tetrahedron Lett.* **1978**, 357–360.
(9) Bingham, R. C.; Schleyer, P. v. R. *Top. Curr. Chem.* **1971**, *18*, 83–87.
(10) Paul, I. C.; Johnson, S. M.; Paquette, L. A.; Barrett, J. H.; Haluska, R. J. *J. Am. Chem. Soc.* **1968**, *90*, 5023–5024.
(11) (a) Parr, R. G. "The Quantum Theory of Molecular Electronic Structure"; W. A. Benjamin: New York, 1963. (b) Two-center repulsion integral (*rr|ss*): Nishimoto, K.; Mataga, N. *Z. Phys. Chem.* (*Frankfurt am Main*) **1957**, *13*, 140–157. (c) Core resonance integral (β_{rs}): Wolsberg. M.; Helmholtz, L. *J. Chem. Phys.* **1952**, *20*, 837–843.
(12) Pople, J. A.; Beveridge, D. L. "Approximate Molecular Orbital Theory"; McGraw-Hill: New York, 1970.

Table II. Stabilization Energies[a] by CNDO/2 MO Calculation

	4	5	5′	3	6
total intercore repulsion	16 335.8	15 959.8	15 982.3	16 787.6	16 708.4
total electronic energy	−20 947.7	−20 551.3	−20 573.8	−21 378.7	−21 298.8
total energy	−4 592.0	−4 591.4	−4 591.4	−4 591.1	−4 590.5

[a] In electron volts.

Table III. Cycloadducts from Cyclopentadienones and *N*-(Ethoxycarbonyl)azepine

compd	ν_{max}, cm^{-1} (C=O)[a]	λ_{max}, nm (ϵ)	mp, °C	*m/e*
3a	1770	226 (16400)[b] 251 (14100)[b]	206–208	513 ([M]$^+$) 165 ([$C_9H_{11}NO_2$]$^+$)
4a	1800	228 (26400)[b]	134–136	
5a	1705	254 (11700)[b] 296 (11800)[b]	155–157	513 ([M]$^+$) 165 ([$C_9H_{11}NO_2$]$^+$)
5d	1725	340 (6500)[c] 400 (4000)[c]	164–166	399 ([M]$^+$)

[a] In Nujol. [b] In ethanol. [c] In benzene.

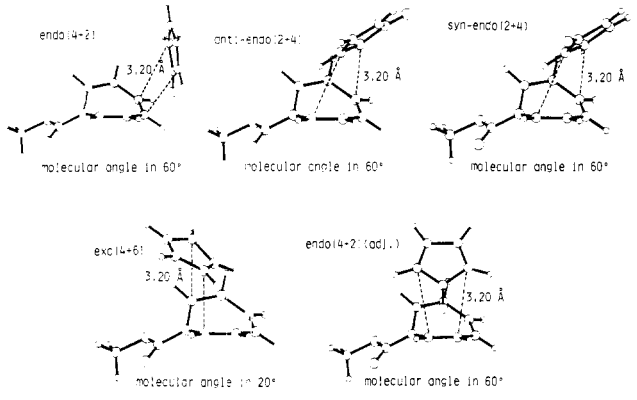

Figure 3. Computer drawing of transition states for various modes of cycloadditions.

for 2,5-dimethyl-3,4-diphenylcyclopentadienone (**1b**) and tetracyclone (2,3,4,5-tetraphenylcyclopentadienone, **1c**) which have often been used as trapping reagents. This predicts that **1a** will show high reactivity to **2a** in comparison with other cyclopentadienones (**1b,c**), and it also predicts a remarkable donor proptery for *N*-(ethoxycarbonyl)azepine (**2a**).

Figure 2 shows the frontier molecular orbitals (FMO) of **1a** and **2b**, wherein the signs of the P_z coefficients are represented by the diameters of the circles at each atom: the interaction of the **1a** LUMO with the **2b** HOMO will be dominant, suggesting acceleration of the reaction rate. Since the sizes of the FMO coefficients are approximately the same magnitude in both cases, confident predictions of periselectivity cannot be made on the basis of the FMO consideration.

The stabilization energies for the cycloaddition reaction of unsubstituted cyclopentadienone (**1f**) with *N*-(methoxycarbonyl)azepine (**2b**) were calculated by treatments with perturbation theory, with the assumption that the two components might approach with molecular angles of 60° for endo addition and of 20° for exo addition[13] as illustrated in Figure 3. The values of the total energies are listed in Table II for a bonding distance of 3.20 Å, for which van der Waals repulsion can be neglected. As shown in Table II, the calculated data suggest that endo adduct (**4**)

(13) (a) Mametsuka, H.; Mori, A.; Takeshita, H.; Yamaguchi, H. In Abstracts of the 9th Congress of Heterocyclic Chemistry, Fukuoka, Japan, 1976, pp 211–215. (b) Herndon, W. C.; Hall, L. H. *Tetrahedron Lett.* **1967**, 3095–3100.

Scheme II

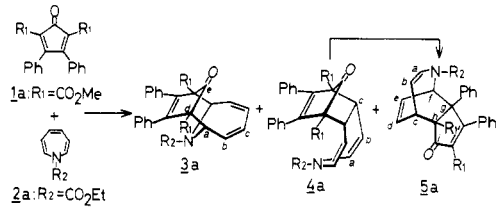

Table IV. ^{1}H NMR Data[a] for Cycloadducts

compd	chemical shifts, δ[b]
3a[c]	5.6–6.5 (m, 6 H, H_a, H_b, H_c)
4a[c]	6.92 (d, 2 H, H_a, J_{ab} = 10), 5.54 (dd, 2 H, H_b, J_{bc} = 3), 3.74 (br s, 2 H, H_c)
5a[c]	6.70 (d, 1 H, H_a, J_{ab} = 9), 6.40 (t, 1 H, H_d, J_{cd} = 6, J_{de} = 7), 5.2–5.8 (m, 3 H, H_b, H_e, H_f), 3.23 (t, 1 H, H_c, J_{bc} = 8)
5d[d]	6.84 (d, 1 H, H_f, J_{ef} = 6), 6.48 (dd, 1 H, H_d, J_{cd} = 7, J_{de} = 8), 6.39 (d, 1 H, H_a, J_{ab} = 7), 5.64 (t, 1 H, H_e), 4.88 (t, 1 H, H_b), 3.45 (t, 1 H, H_c)

[a] Solvent $CDCl_3$. [b] *J* values are given in hertz. [c] See Scheme II for atom labels. [d] See Scheme III for atom labels.

formation is most energetically favorable, while the exo adduct (**3**) formation is energetically unfavorable.

Pericyclic Reactions of 1a with 2a. Heating a mixture of 2,5-bis(methoxycarbonyl)-3,4-diphenylcyclopentadienone (**1a**) and *N*-(ethoxycarbonyl)azepine (**2a**) in benzene at 80 °C for 6 h resulted in the formation of two crystalline products, exo [4 + 6]π cycloadduct **3a** (mp 206–208 °C, yield 17%) and anti endo [2 + 4]π cycloadduct **5a** (mp 155–157 °C, yield 82%), assigned the formula $C_{30}H_{27}NO_7$, which are responsible for the corresponding 1:1 adducts (scheme II).

The infrared (IR) spectrum of **3a** showed a characteristic carbonyl band at 1770 cm^{-1}, suggesting the presence of a bridged carbonyl group. On the other hand, **5a** exhibited IR bands at 1742 and 1732 (ester carbonyl), 1710 (urethane carbonyl), and 1705 (enone carbonyl) cm^{-1} and no absorption due to a strained carbonyl. The ^{1}H NMR spectrum of **3a** exhibited complex absorption bands owing to the nature of the adduct which would be due to nonequivalence resulting from the partial-bond character of the N–C bond. The ^{1}H NMR spectrum of compound **3a** displayed the methylene proton signals of the ethoxycarbonyl group, the methine proton signals, and the olefinic

Table V. ^{13}C NMR Data[a] for Cycloadducts

compd	chemical shifts, δ
3a[b]	58.1 (d, C_a), 70.6 (s, C_d), 119.0 (d, C_c), 131.8 (d, C_b), 193.8 (s, C_e)
5a[b]	30.1 (d, C_c), 53.3 (s, C_g), 73.2 (s, C_h), 109.6 (d, C_b), 134.5 (d, C_a), 197.6 (s, C_i)
5d[c]	38.9 (d, C_c), 69.0 (d, C_f), 80.2 (s, C_g), 108.6 (d, C_b), 134.0 (d, C_a), 201.0 (s, C_h)

[a] Solvent $CDCl_3$. [b] See Scheme II for atom labels. [c] See Scheme III for atom labels.

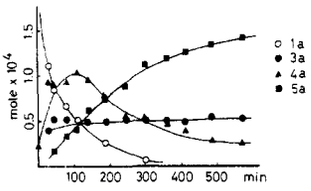

Figure 4. Rate of reaction of 2,5-bis(methoxycarbonyl)-3,4-diphenylcyclopentadienone (**1a**) with *N*-(ethoxycarbonyl)azepine (**2a**) in $CDCl_3$ at 43 °C.

proton signals as a doubling up of signals and as analyzable signals at 80 °C in C_6D_6 solution, respectively.

By contrast, the ^{13}C NMR spectrum (14.59, 52.38, 58.01, 58.18, 62.34, and 70.55 ppm) of **3a** suggested a symmetrical structure. In the case of **5a**, the ^1H NMR and ^{13}C NMR spectra were difficult to analyze precisely because of the number of overlapping resonances. In order to elucidate the complete stereostructure of these adducts, we carried out the crystal structure analyses as described below. The physical data of these adducts (**3a**, **5a**) are summarized in Tables III–V.

On the other hand, **1a** and **2a** reacted at room temperature to give **3a** and a 1:1 cycloadduct (**4a**). The IR spectrum of **4a** showed a strained carbonyl band at 1800 cm^{-1}. The ^1H NMR spectrum of **4a** revealed the presence of two protons as a slightly broadened singlet absorption at δ 3.74, two vinyl protons β to nitrogen as a doublet ($J \simeq 3$ Hz with additional small coupling) at δ 5.54, and two vinyl protons α to nitrogen as a doublet ($J = 10.4$ Hz) at δ 6.91. The symmetry of **4a** was apparent. The physical data of **4a** are summarized in Tables III and IV.

When **1a** and **2a** were dissolved in $CDCl_3$ at 43 °C, monitoring of the ensuing reaction by analyzing the ^1H NMR signals of the OMe groups of **1a** at δ 3.64, **3a** at δ 3.51 and 3.59, **5a** at δ 2.88, and **4a** at δ 3.62 revealed the initial formation of **4a**. As illustrated by Figure 4, the concentration of **4a** increased rapidly until a maximum was reached (2.0 h) and then decreased gradually with the increase of **5a**. From the consumption of **4a** and the behavior of the other compositions (**1a** and **3a**), it is obvious that **4a** is converted to **5a**.

Cycloaddition Reaction of 1d with 2a. Thermolysis of 1,3-bis(diazo)-1,3-diphenyl-2-propanone (**8**) provided a simple route to 2,5-diphenyl-3,4-diazacyclopentadienone (**1d**) which is obtained as a convenient and a powerful electron-deficient heterodiene component in spite of an unstable intermediate (Scheme III). Indeed, this fascinating intermediate has been shown to act as both a dienophile with 2,3-dimethyl-1,3-butadiene and a diene with norbornene in the pericyclic reactions.[14] These interesting features of the pericyclic reactions of diazacyclopentadienone **1d** prompted us to examine the model of cycloaddition of **8** with *N*-(ethoxycarbonyl)azepine (**2a**):

Scheme III

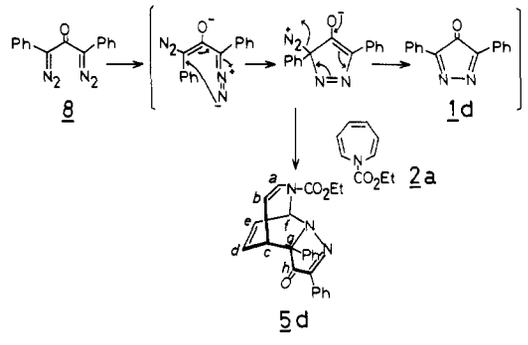

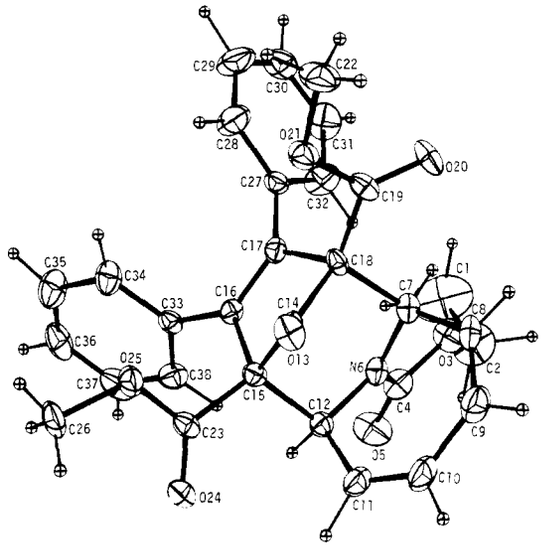

Figure 5. ORTEP drawing of exo [4 + 6]π cycloadduct **3a**.

1d reacted rapidly with **2a** to give a 1:1 cycloadduct (**5d**) in a moderate yield (Scheme III).

The ^{13}C NMR spectrum in C_6D_6 of **5d** showed five detectable signals of sp^3 carbons, of which signals at 38.85, 68.96, and 80.16 ppm are ascribable to the structure of the [2 + 4]π cycloadduct. The UV absorption at λ_{max} (benzene) 400 nm (ε 4000) is in good agreement with that expected for the conjugated chromophore (N=C—C=O).

From these data, the structure of **5d** was considered to be that of a [2 + 4]π cycloadduct instead of a [4 + 6]π cycloadduct. However, there is some obscurity in the regiochemistry of **5d**. Assignment of the conjugated carbonyl absorption at 1725 cm^{-1} by IR spectroscopy is uncertain for that expected structure. Thus, **5d** was submitted to single-crystal X-ray analysis as described below. The physical data of **5d** are summarized in Tables III–V.

Cope Rearrangement of Cycloadduct 4a. The UV spectrum of **4a** after the sample was allowed to stand at 34.1 °C in ethanol for 3 days agrees with that of **5a**. The reaction rate was determined by measuring the increase of the absorbance at 300 nm due to an enone conjugated with phenyl group. In this solvent satisfactory first-order behavior of the reaction was observed. The rate constants ($10^4 k_1$ s^{-1}) of the Cope rearrangement at various temperatures are as follows: at 34.1 °C, 0.54; at 40.0 °C, 2.36; at 47.8 °C, 4.50; at 58.9 °C, 12.5. The kinetic parameters of the Cope rearrangement were calculated in a usual manner from these rate constants: $E_a = 24.2 \pm 1.0$ kcal mol^{-1} and $\Delta S^{\ddagger} = -0.64 \pm 3.0$ eu (at 47.8 °C).

Crystallographic Study. As described above, the ^1H NMR and ^{13}C NMR spectra of these adducts (**3a**, **5a**, and **5d**) were difficult to analyze precisely because of the large

(14) Trost, B. M.; Whiteman, P. J. *J. Am. Chem. Soc.* **1974**, *96*, 7421–7428.

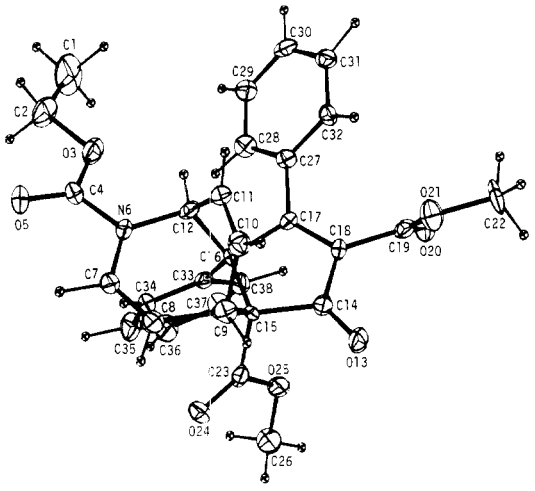

Figure 6. ORTEP drawing of anti endo [2 + 4]π cycloadduct **5a**.

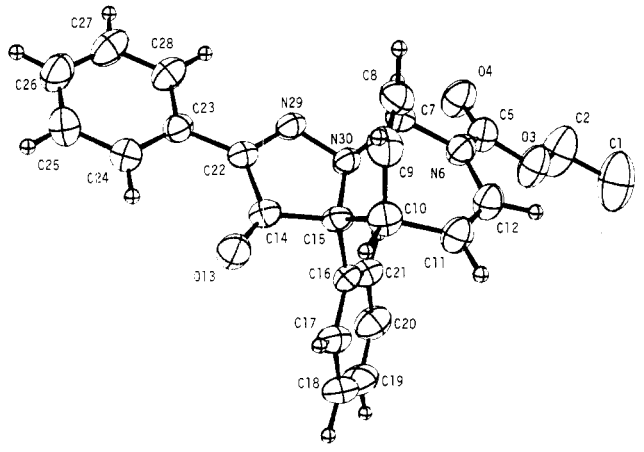

Figure 7. ORTEP drawing of anti endo [2 + 4]π cycloadduct **5d**.

number of overlapping resonances. In order to elucidate the complete stereostructure of the cycloadducts and to account for the spectroscopic data, we carried out crystallographic analyses.

The configurations of the adducts (**3a**, **5a**, and **5d**) with the numbering sequence in this paper are illustrated in Figures 5–7, respectively, where each atom is represented as an ellipsoid with 20% probability.

Of the Cycloadduct 3a. As can be seen in the computer-generated drawing (Figure 5), the molecular structure of **3a** was confirmed as an exo [4 + 6]π cycloadduct. The tricyclo[6.2.1.1]dodecan-11-one moiety is strained considerably. In the absence of strain, the bond angle of C–CO–C would be ca. 120°, but this angle is reduced to 102.9 ± 0.6°. This agrees with the IR band for the carbonyl at 1770 cm^{-1}. The C_{12}–C_{15} and C_7–C_{18} bond lengths, 1.58 and 1.61 Å, respectively, are considerably longer than the usual value, 1.54 Å. These unusually long bond distances might be caused by large steric repulsions between the planes of the cyclopentadienone moiety and the 1*H*-azepine moiety.

Of the Cycloadduct 5a. As shown in Figure 6, the molecular structure of **5a** is established to be that of an anti endo [2 + 4]π cycloadduct wherein the regiochemistry of the carbonyl to the urethane group is an anti orientation. The framework of **5a**, which consists of the 1*H*-azepine and cyclopentadienone moieties, is strained considerably. The C_7–C_{16} bond length, 1.58 Å, is considerably longer than the usual value, 1.54 Å. This long bond distance might be caused by large steric repulsions between the 1*H*-azepine moiety and the phenyl group of **1a**. The nitrogen atom N_6 deviates by 0.046 Å from the plane of the three atoms bonded to it, indicating sp^2 hybridization. The N_6–C_{12} bond (1.39 Å) is shorter than the accepted value for a N–C single bond, e.g., N_6–C_7 (1.48 Å). The torsional angles O_5–C_4–N_6–C_{12}, C_{11}–C_{12}–N_6–C_4, N_6–C_{12}–C_{11}–C_{10}, C_7–N_6–C_{12}–C_{11} are 7.3°, 6.5°, 2.8°, and 0.3°, respectively. These facts suggest that the atoms C_4, O_5, N_6, C_7, C_{10}, C_{11}, and C_{12} are roughly planar, forming a resonance structure of the vinyl urethane, and this supports the IR and UV spectral data as described above. The C_8–C_{17} distance, 2.82 Å, is considerably short, suggesting the possibility of photochemical conversion of **5a** to a cage compound.[7]

Of the Cycloadduct 5d. The molecular structure shown in Figure 7 established that **5d** has the structure of an anti endo [2 + 4]π cycloadduct from **1d** (2π) and **2a** (4π).

The C_{15}–C_{14}–C_{22} angle is 4° smaller in the diazacyclopentadienone **1d** than in the cyclopentenone.[15] This difference might be due to the short bond distance of the N–N bond of **1d** as compared with a corresponding cyclopentenone, which gave rise to a higher C=O stretching frequency at 1725 cm^{-1} in the IR spectrum.

In consideration of the molecular structure of **5d**, we can consequently explain the ^1H NMR spectrum by spin–spin decoupling experiments and study of the solvent-induced shifts of the resonance of the olefinic protons. The six methine protons in the ^1H NMR spectrum ($CDCl_3$ with tetramethylsilane as internal standard) are ascribed as summarized in Tables III–V.

Discussion

As shown in Figure 1, 2,5-bis(methoxycarbonyl)-3,4-diphenylcyclopentadienone (**1a**) should more readily react with *N*-(ethoxycarbonyl)azepine (**2a**) than the other cyclopentadienones such as 2,5-dimethyl-3,4-diphenylcyclopentadienone (**1b**) and tetracyclone (**1c**). Indeed, **1a** readily reacted with **2a** under milder conditions (room temperature) in comparison with the case of **1b**.[16]

From the calculated FMO energy levels of **1b** and **1c** qualitative similarities in reactivity between the two compounds are expected, but there is large difference in reactivity between **1b** and **1c**: **1b** reacts with dienophiles much faster than **1c**. The difference in reactivity between them may be accounted for by consideration of steric repulsions between reactants. As a phenyl group is more bulky than a methyl group, **1c** shows lower reactivity than **1b**.

Comparison of the ^1H NMR spectra of the endo [4 + 2]π cycloadduct (**4a**) and the analogous cycloadduct (**10**) of **1b** and **2a** revealed that the protons α to the nitrogen of **4a** have undergone an upfield shift relative to those of **10**.[16] This fact indicates the existence of the phenyl ring-current effect on the protons α to nitrogen, suggesting the endo [4 + 2]π structure for **4a** and suggesting that the conformation of **4a** is preferable to that of **10** for the Cope rearrangement. There are two alternative analyses by which reactivity in the [3,3] sigmatropic shifts may be predicted: the radical union approach and the reactant dissection method.[17a] The former uses the two odd radical fragments which make up the transition state of the reaction and considers the effect of substituents on the interactions of these two fragments.[17b] The latter utilizes

(15) Harano, K.; Ban, T.; Yasuda, M.; Kanematsu, K. *Tetrahedron Lett.* **1978**, 4037–4038.
(16) Paquette, L. A.; Kuhla, D. E.; Leichter, L. M. *J. Org. Chem.* **1969**, *34*, 2888–2896.
(17) (a) Houk, K. N. "Pericyclic Reactions"; Academic Press: New York, 1977; pp 248–255. (b) Ingaki, S.; Fujimoto, H.; Fukui, K. *J. Am. Chem. Soc.* **1976**, *98*, 4693–4701.

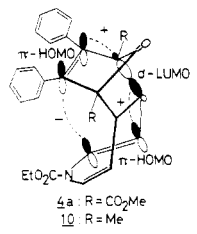

Figure 8. Three-system interactions for the Cope rearrangement.

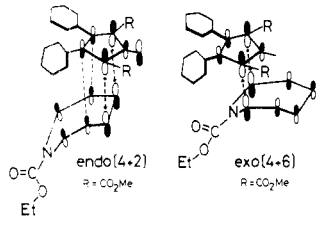

Figure 9. Frontier orbitals and secondary interactions for the cycloaddition of **1a** to **2a**.

a dissection of the reactants into σ and π fragments and a consideration of the effect of substituents on the interaction of the frontier orbitals of the two fragments. Thus, it seems plausible that the interaction among the HOMO's of the two π bonds and LUMO of the σ bond for **4a** in comparison with the case of **10** could be preferred for the rearrangement: a cyclic (HOMO, LUMO, HOMO) interaction is depicted in Figure 8. The methoxycarbonyl group lowers the σ LUMO, whereas the methyl and the enamine one raises the σ LUMO and the π HOMO, respectively. Thus, the FMO interaction becomes quite favorable. In case of **4a**, HOMO–LUMO energy gaps between the π bond and the σ bond decrease, resulting in the rate enhancement.[5]

As described above, it has been firmly established that the reaction of **1a** with **2a** leads to exo [4 + 6]π and anti endo [2 + 4]π cycloadducts.

With respect to the regiochemistry of the pericyclic reaction, two [2 + 4]π regioisomers (**5** and **5'**) may be derived from the independent pathway, and the interconversion of these isomers cannot be allowed under the thermal conditions.

The ^{1}H NMR monitoring data as shown in Figure 4 suggest that anti endo [2 + 4]π cycloadduct **5a** is the result of the Cope rearrangement[3,5,16] of the alternative endo [4 + 2]π cycloadduct **4a** in which **1a** acts as the diene, while exo [4 + 6]π cycloadduct **3a** forms directly.

The transition state for the formation of **3a** might be similar to that of **4a** as shown in Figure 9. The formation of [4 + 6]π cycloadduct **3** might be controlled by the antibonding secondary interactions of the frontier orbitals and the dipole–dipole interaction between the reactants in the transition state, and the preferential formation of the endo [4 + 2]π adduct **4** can be rationalized in terms of the secondary orbital interactions (bonding) in the transition state.

Recently several reports[18a] concerning the cycloaddition of cyclic trienes such as tropone and cycloheptatriene to suitable dienes in a [4 + 6]π reaction have appeared.

However, there are two reports concerning the isolation of [4 + 6]π cycloadduct **3** from 1*H*-azepine and dienes under more drastic reaction conditions in very low yield.[6,18b]

(18) (a) Mukherjee, D.; Watts, C. R.; Houk, K. N. *J. Org. Chem.* **1978**, *43*, 817–821 and references cited therein. (b) Iida, S.; Mukai, T. *Heterocycles* **1978**, *11*, 401–408.

This difference might be attributed to the presence of a more bulky group, the *N*-ethoxycarbonyl group, at the triene termini.

As shown in Table II, the intercore repulsion term is the largest in the case of exo adduct **3**, resulting in destabilization of the transition state for the formation of **3**. There is a necessity for a closer consideration of the actual geometrical relationship of the cycloaddition reaction.

Thus, inspection of a Dreiding model suggests that cyclopentadienone approaching with a molecular angle of 20°[13] to the plane defined by the two π bonds adjacent to the N atom would encounter major steric hindrance between the substituents of the cyclopentadienone and the *N*-ethoxycarbonyl group of **2a**, where little bonding can have developed compared with the cases of other seven-membered-ring polyenes, e.g., tropone. In fact, the cycloadditions of phencyclone (**1e**) and 2,5-dimethyl-3,4-diphenylcyclopentadienone (**1b**) with *N*-(ethoxycarbonyl)azepine (**2a**) gave the peri- and stereospecific endo [4 + 2]π cycloadducts **4**.[3,16]

By contrast, as stated above, the cycloaddition of **1a** with **2a** gave a novel [4 + 6]π cycloadduct in moderate yield.

When more bulky groups such as the phenyl moiety are substituted at the 2,5-positions of 3,4-diphenylcyclopentadienone, each group is forced to lie in a nearly perpendicular disposition with respect to the plane of cyclopentadienone, owing to the van der Waals repulsions wherein the secondary orbital interactions of the FMO are unfavorable, thus effecting the destabilization of the transition state of endo [4 + 2]π cycloadduct formation.

Finally, stereospecific formation of anti endo [2 + 4]π cycloadduct **5d** suggests that **5d** was formed via Cope rearrangement of the corresponding endo [4 + 2]π cycloadduct **4d** in the same fashion as in the case of **1a**.

Experimental Section

The melting points were measured with a Yanagimoto micro melting point apparatus and are uncorrected. The UV spectra were determined with a Hitachi EPS-3T spectrophotometer. The ^{1}H NMR spectra were taken with a JEOL PS-100 spectrometer with Me_4Si as an internal standard, and the chemical shifts are expressed in δ values. The IR spectra were taken with a JASCO IR A-1 infrared spectrophotometer. Mass spectra were obtained with a JEOL JMS-01SG double-focusing spectrometer operating at an ionization potential of 75 eV. The solid samples were ionized by electron bombardment after sublimation directly into the electron beam at 150–200 °C.

Cycloaddition Reaction of 2,5-Bis(methoxycarbonyl)-3,4-diphenylcyclopentadienone (1a) with *N*-(Ethoxycarbonyl)azepine (2a). A solution of **1a** (3.24 g) and **2a** (3.30 g) in benzene (30 mL) was heated at 80 °C for 6 h. The solvent was then evaporated under reduced pressure, and the residue was chromatographed on silica gel with *n*-hexane–benzene (5:1). The first fractions gave **3a** (0.81 g, 17%) as colorless prisms, and the second fractions gave **5a** (3.90 g, 82%) as pale yellow needles. The results are summarized in Tables III–V.

On the other hand, **1a** (0.17 g) and **2a** (0.30 g) were dissolved in benzene (1 mL). After the solution was allowed to stand overnight at room temperature, *n*-hexane was added, and the precipitated solid (140 mg) was filtered off. From the mixture, **4a** (0.01 g) was obtained by manual picking up of the colorless prisms. The results are summarized in Tables III–V.

Cycloaddition Reaction of 1,5-Diphenyl-3,4-diazacyclopentadienone (1d) with 2a. A solution of 1,3-bis(diazo)-1,3-diphenyl-2-propanone (**8**, 1.6 g) and **2a** (1.2 g) in benzene (10 mL) was stirred overnight at room temperature. Evaporation of benzene and column chromatography over silica gel (*n*-hexane–ethyl acetate, 1:1) gave 1.14 g (47.5%) of **5d**. The results are summarized in Tables III–V.

Cope Rearrangement of Endo [4 + 2]π Cycloadduct 4a to Anti Endo [2 + 4]π Cycloadduct 5a. A solution of **4a** (0.2 g) in benzene (2 mL) was heated at 80 °C for 2 h. The solvent was

Table VI. Summary of Crystal Data and Intensity Collection

	3a	5a	5d
formula	$C_{30}H_{27}NO_7$	$C_{30}H_{27}NO_7$	$C_{24}H_{21}N_3O_3$
mp, °C	206–208	155–157	164–166
geometry	monoclinic	triclinic	triclinic
a, Å	16.447 (6)	11.069 (14)	9.920 (3)
b, Å	9.933 (4)	20.690 (23)	12.503 (5)
c, Å	16.331 (6)	10.579 (10)	9.172 (3)
α, deg		114.03 (8)	107.20 (3)
β, deg	100.53 (3)	100.06 (9)	105.46 (2)
γ, deg		130.97 (7)	98.26 (3)
cryst vol, Å^3	2623 (2)	1283 (2)	1016 (1)
space group	$P2_1/c$	$P\bar{1}$	$P\bar{1}$
Z	4	2	2
density[a] calcd, g/cm^3	1.320	1.326	1.252
exptl, g/cm^3	1.296	1.330	1.263
solvent	methanol	ethanol	acetone
temp, °C		20	
radiation		Mo Kα (λ = 0.710 69 Å)	
scan speed, deg/min		24.0–4.0	
scan range, deg		$2\theta \leq 55$	
unique data collected	3940	3970	3530
unique data used ($I > 2.5\sigma(I)$)	1956	1424	2792

[a] KI + H_2O.

evaporated under reduced pressure, and the residue was recrystallized from ethanol to give **5a** (0.198 g) quantitatively as pale yellow needles.

Kinetics. The rates of rearrangement of **4a** were followed at a given temperature by the increase of enone absorption at 300 nm by using a 10 × 10 mm quartz cell which was thermostated with flowing water at constant temperature. The first-order rate constants (k_1) were calculated from a plot of $\ln (A_t - A_\infty)/(A_0 - A_\infty)$ vs. time by means of the least-squares method, where A_t is the absorbance at time t and A_∞ is the absorbance after 10 half-lives.

X-ray Crystallography. (A) Exo [4 + 6]π Cycloadduct 3a. Single crystals of the compound **3a** were prepared by slow evaporation of a methanol solution at room temperature. The density was measured by flotation in an aqueous potassium iodide solution.

The cell constants were found by a least-squares procedure using the values of the Bragg angles of 15 reflections. Systematic absences for the $h0l$ reflections with $l = 2n + 1$ and for the $0k0$ reflections with $k = 2n + 1$ are consistent with the space group $P2_1/c$.

Intensity data were collected on a Syntex $P\bar{1}$ automated diffractometer with Mo Kα radiation monochromated with a graphite crystal and by using θ–2θ scans to a limit of $2\theta = 55°$. A variable scan rate from 24.0 to 4.0°/min was used. Three reflections were monitored after every measurement of 97 reflections. Of 3940 independent reflections, 1956 were treated as observed ($I > 2.5\sigma(I)$). The intensities were corrected for Lorentz and polarization effects, but no correction was applied for absorption. The data are summarized in Table VI. .

Observed structure factors were converted into normalized structure factor amplitude values ($|E|$) by use of a scale factor and the overall temperature factor obtained from Wilson's statistics.[19] The structure was solved by the direct method using the MULTAN series of programs.[20] An E map calculated with 292 signed E's ($|E| \geq 1.60$), which gave an absolute figure of merit of 1.432, revealed the positions of 36 of the nonhydrogen atoms. The positions of the remaining two atoms were located on a subsequent difference Fourier map. Six cycles of block-diagonal least-squares minimizing of $\sum(|F_o| - k|F_c|)^2$ by varying the positions and isotropic vibrational amplitudes of the C, N, and O atoms led to $R = 0.134$. Nine further cycles of least-squares refinement of atomic parameters with anisotropic vibrational amplitudes for the all atoms converged to $R = 0.102$. Twenty-two of the 27 hydrogens were located from a difference electron density map. The positions of the remaining five, bonded to carbon atoms with high thermal parameters, were calculated by using the program HYCO.[21]

After adding the hydrogens, keeping their vibrational amplitudes fixed (B(H) = B(C) + 1.0 Å), and refining the values with anisotropic U's for all C, N, and O atoms, we obtained a final R of 0.077.

(B) Anti Endo [2 + 4]π Cycloadduct 5a. The data collection, phasing, and refinement for **5a** were carried out in almost the same manner as for **3a** (Table VI).

An E map calculated with 262 signed E's ($|E| \geq 1.7$), which gave an absolute figure of merit of 1.1371, revealed the positions of 37 of the nonhydrogen atoms.

A subsequent difference Fourier map and several cycles of refinement with isotropic and then anisotropic temperature factors resulted in the discrepancy factor $R = 0.098$ for the observed reflections. The hydrogen atoms were placed in calculated positions. Refinement was terminated at $R = 0.073$.

(C) Anti Endo [2 + 4]π Cycloadduct 5d. The crystallographic procedures were the almost the same as those described above (Table VI).

The orientation of the major part of the molecule was found by direct phasing[20] (absolute figure of merit of 1.0859), but difficulty was experienced in finding a correct phasing model owing to two overlapping molecules. The middle positions of both models were used for phase determination (29 atoms). The position of the remaining atom was obtained from a difference Fourier map. Refinements were carried out by the block-diagonal least-squares method using isotropic temperature factors for the hydrogen atoms, with the exception of the hydrogen atoms of the ethyl group with high temperature factors, and anisotropic temperature factors for the remaining atoms. The final R value was 0.053 for the observed reflections.

All calculations were performed on the FACOM M-190 computer in the computer center of Kyushu University with the Universal Crystallographic Computation Program System (UNICS II).[21] Atomic scattering factors were taken from ref 22. Observed structure amplitudes and structure factors calculated from the final atomic coordinates are listed in Tables VII–IX (supplementary material).

Acknowledgment. The authors are grateful to Professor I. Ueda and Assistant Professor S. Kawano (College

(19) Ashida, T. "SIGMA. The Universal Crystallographic Computing System"; The Crystallographic Society of Japan: Tokyo, Japan, 1967; Part I, pp 43, 44.

(20) Germain, G.; Main, P.; Woolfson, M. M. *Acta Crystallogr., Sect. A* **1971**, *A27*, 368–376.

(21) Sakurai, T.; Iwasaki, J.; Kobayashi, K.; Bando, Y.; Nakamichi, Y. *Rikagaku Kenkyusho Hookoku* **1974**, *50*, 74–91.

(22) "International Tables for X-ray Crystallography"; Kynoch Press: Birmingham, England, 1974; Vol. 4, pp 72–98.

of General Education, Kyushu University) for providing their X-ray crystallographic programs.

Registry No. 1a, 16691-79-5; 1b, 26307-17-5; 1c, 479-33-4; 1d, 32683-51-5; 1e, 5660-91-3; 1f, 13177-38-3; 2a, 2955-79-5; 2b, 17870-94-9; 3, 74947-87-8; 3a, 72001-25-3; 4a, 74947-88-9; 5', 74947-89-0; 5a, 72003-84-0; 5d, 70363-69-8; 6, 74947-90-3; 8, 26536-34-5; 9, 106-99-0.

Supplementary Material Available: Listings of interatomic distances (Table X, 3a; Table XI, 5a; Table XII, 5d), intermolecular angles (Table XIII, 3a, Table XIV, 5a; Table XV, 5d), atomic and anisotropic thermal parameters (Table XVI, 3a; Table XVII, 5a; Table XVIII, 5d), and hydrogen atomic parameters (Table XIX, 3a; Table XX, 5a; Table XXI, 5d) (12 pages). Ordering information is given on any current masthead page.

Photocycloaddition Chemistry of 2-(Trimethylsilyl)cyclopentenone and 5-(Trimethylsilyl)uracil. The Utility of a Trimethylsilyl Group as a Removable Directing Group in Photochemistry

Chuan Shih,[1] Edward L. Fritzen,[2] and John S. Swenton*

Department of Chemistry, The Ohio State University, Columbus, Ohio 43210

Received June 6, 1980

The photocycloaddition reactions of 2-(trimethylsilyl)cyclopentenone with isobutylene, methylenecyclohexane, isopropenyl acetate, propylene, and propyne were investigated. In the first three cases, a regiospecific reaction giving the head-to-tail photoadduct was observed while with propylene and propyne a mixture of head-to-head and head-to-tail isomers was produced. The directing effect of the 5-trimethylsilyl group in uracil photocycloaddition chemistry was dramatic; isobutylene, methylenecyclohexane, and even propylene gave only the head-to-tail adduct in high yield. These photoaddition products may be desilylated to adducts of cyclopentenone and uracil by potassium fluoride dihydrate in dimethyl sulfoxide. The reactions of 2-(triethylsilyl)- and 2-(triphenylsilyl)-cyclopentenone with propene were briefly examined to evaluate the effect of silicon substituents on the regioselectivity of the photocycloaddition reaction. The reaction of the former system with propene gives approximately the same ratio of photocycloaddition products as 2-(trimethylsilyl)cyclopentenone. Attempted photochemical reactions with 2-(triphenylsilyl)cyclopentenone led to decomposition of the starting enone. Finally, the use of a stannous chloride filter solution or a uranium glass filter for cyclopentenone photocycloaddition reactions minimizes the problem of secondary irradiation products being formed in these additions.

Introduction

Since the early observations of intramolecular photoaddition of cyclic enones to double bonds[3] and the extension of these reactions to intermolecular examples,[4,5] such cyclobutane-forming reactions have been of extensive value in organic syntheses. Thus, key steps in the synthesis of caryophyllene,[5] α-caryophyllene alcohol,[6] β-himachalene,[7] bourbonene,[8] loganin,[9] and ormosanine[10] involved photocycloaddition of an α,β-unsaturated ketone to olefin systems. Besides these classic examples, the recent literature is replete with new applications of these reactions in organic synthesis.

In spite of much effort in this area, there is still no clear picture of all the factors involved in determining the stereochemistry of the cyclobutane-ring fusion or the regioselectivity of cycloaddition reactions on unsymmetrical substrates.[11] However, the absence of mechanistic understanding of these reactions is countered by a wealth of literature examples[12] which allows certain generalizations to be made. First, the photocycloaddition reactions of cyclohexenones to oxygenated olefins (i.e., enol acetates, enol ethers, and ketene acetals) usually proceed in a highly selective head-to-tail manner. Second, the photocycloaddition reactions of cyclic enones with olefins bearing certain conjugating groups [i.e., >C=CR(CO_2CH_3)] give predominantly head-to-head products. However, the reactions of cycloalkenones (cyclohexenone, cyclopentenone) with simple unsymmetrical olefins often give rise to complications. While examples of such reactions are less numerous in the literature—presumably due to complications involved in the separation and characterization of the products—an ample number of reports attests to the low regioselectivity of the reaction.[5,8,12,13] In spite of the problem of mixtures of regioisomers encountered in some reactions, the utility of these reactions in some lengthy synthetic procedures[5] attests to the power of the synthetic method.

Scheme I. Proposed Sequence for Regiospecific Photocycloaddition

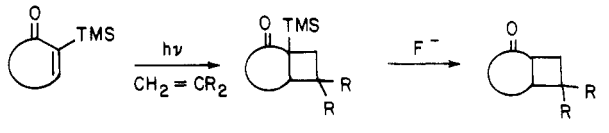

The development of methods for effecting high-yield, regiospecific photocycloadditions of cyclic enones to simple unsymmetrical olefins is an old but important problem. In general α-substituents (i.e., acetoxy,[14] fluoro,[15] methyl[16])

(1) Abstracted in part from M.S. theses of E. L. Fritzen, 1978, and Chuan Shih, 1979, The Ohio State University.
(2) A preliminary report has appeared: Fritzen, E. L.; Swenton, J. S. *Tetrahedron Lett.* **1979**, 1951-1954.
(3) Ciamician, G.; Silber, P. *Chem. Ber.* **1908**, *41*, 1928-1935. Sernaggiotto, E. *Gazz. Chim. Ital.* **1917**, *47*, 153-159; *Ibid.* **1918**, *48*, 52-60. Büchi, G.; Goldman, I. M. *J. Am. Chem. Soc.* **1957**, *79*, 4741-4748.
(4) (a) Eaton, P. E. *J. Am. Chem. Soc.* **1962**, *84*, 2344-2348; (b) *Ibid.* **1962**, *84*, 2454-2455.
(5) (a) Corey, E. J.; Mitra, R. B.; Uda, H. *J. Am. Chem. Soc.* **1963**, *85*, 362-363; *Ibid.* **1964**, *86*, 485-492. (b) Corey, E. J.; Bass, J.; LeManiew, R.; Mitra, R. *Ibid.* **1964**, *86*, 5570-5583.
(6) Corey, E. J.; Nozoe, S. *J. Am. Chem. Soc.* **1964**, *86*, 1652-1653.
(7) Challand, B. D.; Hikino, H.; Kornes, G.; Lange, G.; deMayo, P. *J. Org. Chem.* **1969**, *34*, 794-806.
(8) White, J. D.; Gupta, D. N. *J. Am. Chem. Soc.* **1966**, *88*, 5364-5365.
(9) Büchi, G.; Carlson, J. A.; Powell, J. E.; Fietze, L. F. *J. Am. Chem. Soc.* **1970**, *92*, 2165-2167.
(10) Hunter, N. R.; MacAlpine, G. A.; Liu, H. J.; Valenta, Z. *Can. J. Chem.* **1970**, *48*, 1440-1445.
(11) Wagner, P. J.; Bucheck, D. *J. Am. Chem. Soc.* **1969**, *91*, 5090-5097; *Ibid.* **1970**, *92*, 181-185. For a recent discussion and leading references, see: Loutfy, R. O.; deMayo, P. *Ibid.* **1977**, *99*, 3559-3565.
(12) For a review, see: Meier, H. *Methoden Org. Chem. (Houben-Weyl)* **1975**, *4/5b*, 898-941.
(13) Eaton, P. E. *Acc. Chem. Res.* **1967**, *1*, 50-57.

0022-3263/80/1945-4462$01.00/0